

Electronic Supplementary Information

Investigation of CO₂ Single-Pass Conversion in a Flow Electrolyzer

Emily Jeng and Feng Jiao*

Center for Catalytic Science & Technology, Department of Chemical and Biomolecular Engineering, University of Delaware, Newark, DE 19716, USA

*Corresponding author: jiao@udel.edu

Table of Contents

ESI Table 1: Literature comparison of single-pass conversion in CO₂ electrolyzers

ESI Table 2: Constants for CO₂ to carbonate calculation

ESI Figure 1: SEM image of 100 nm silver nanoparticles deposited on the gas diffusion layer

ESI Figure 2: Serpentine flow field used for the cathode during testing

ESI Method: Calculation of theoretical rate of CO₂ conversion to carbonates

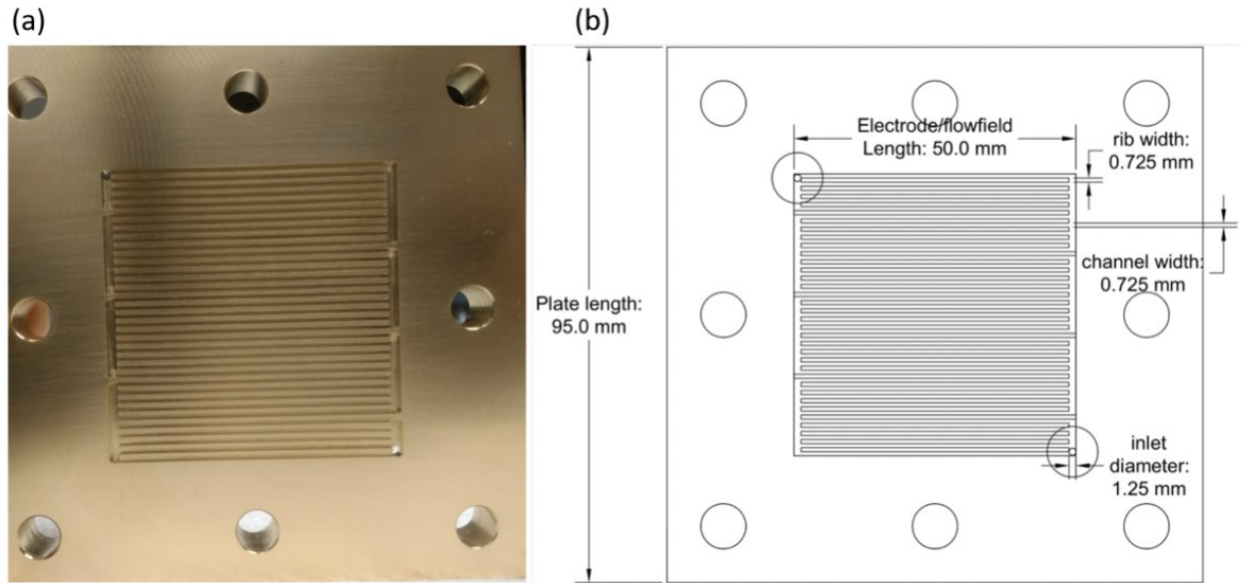
References

ESI Table 1: Literature comparison of CO₂ single-pass conversion in CO₂ flow electrolyzers.

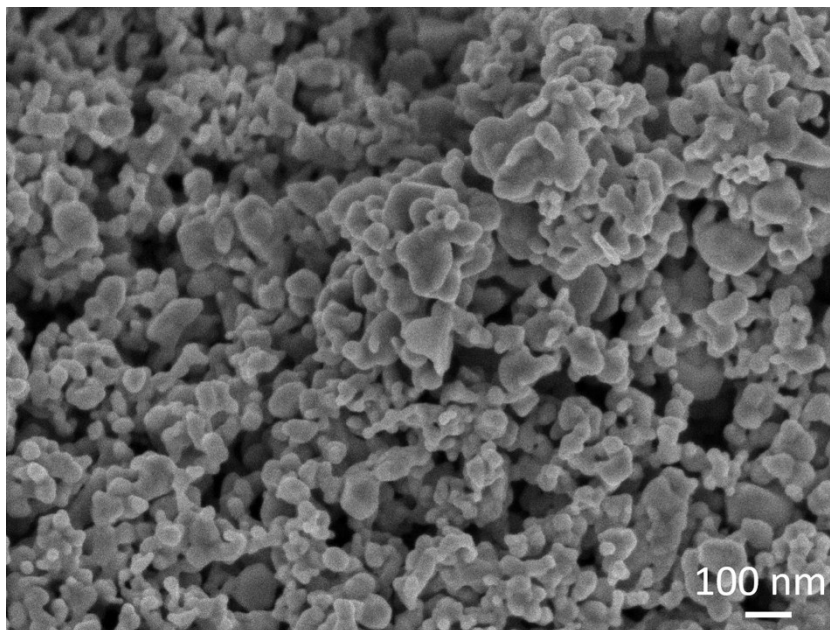
Ref.	Flow cell configuration	Catalyst	CO ₂ feeding rate [mL/min]	Electrode size [cm ²]	CO Faradaic Efficiency [%]	Reported Current Density [mA/cm ²]	Conversion to CO [%]
1	microfluidic flow cell	commercial silver nanoparticles (100 nm)	17	6.25	90%	440	19.7
2	pressurized electrolytic cell	Porous Ag sheet	50	6.25	80-90%	191.25	8.1
3	microfluidic flow cell	Ag/MWCNT on GDL (mixed 1:1)	7	1	90%	350	38.0
4	microfluidic flow cell	MWNT/PyPBI/Au	17	8.4	63.60%	200	44.7
5	microfluidic flow cell	Ag nanoparticles and 40% Ag/TiO ₂	7	1	90%	100	10.9
6	microfluidic flow cell	Ni-N-C	50	5	85%	200	9.1
7	bipolar membrane	Ag nanopowder	100	1	50%	200	9.5
8	liquid flow cell	Ag nanopowder	50	0.1	37%	100	6.1
9	Three-compartment flow cell	Ag nanoparticles	50	3	80%	300	4.6
10	Three-compartment flow cell	Ag/PTFE	50	6.25	90%	150	2.3

ESI Table 2: Constants for the calculations of CO₂ consumption due to carbonate formations.

Constant	Equation/Value	Units	Reference
H_{CO_2}	$34 \times 10^{-6} \exp\left[\left(\frac{1}{T} - \frac{1}{273.15}\right)\right]$	mol cm ⁻³ atm ⁻¹	11
K_1	$10^{[-126.3408 + \frac{6320.813}{T} + 19.568224 \ln(T)]}$	mol cm ⁻³ atm ⁻¹	12
K_2	$10^{[-90.18333 + \frac{5143.692}{T} + 14.613358 \ln(T)]}$	mol cm ⁻³ atm ⁻¹	12
k_{1f}	$2.0 \times 10^{18} \exp\left[-\frac{7698}{T}\right]$	cm ³ mol ⁻¹ s ⁻¹	13
k_w	1.0×10^{-6}	mol cm ⁻³ s ⁻¹	11
D_{OH^-}	$2.89 \times 10^{-5} \exp\left[-1750\left(\frac{1}{T} - \frac{1}{273.15}\right)\right]$	cm ² s ⁻¹	13
$D_{HCO_3^-}$	$7.016 \times 10^{-5} \left(\frac{T}{204.0282} - 1\right)^{2.3942}$	cm ² s ⁻¹	13
$D_{CO_3^{2-}}$	$5.447 \times 10^{-5} \left(\frac{T}{210.2646} - 1\right)^{2.1929}$	cm ² s ⁻¹	13
IEC	1.1×10^{-3}	mol g ⁻¹	14
ρ_{mem}	1.23	g cm ⁻³	15



ESI Figure 1: Serpentine flow field used for the cathode during testing: (a) picture and (b) drawing with dimensions.



ESI Figure 2: SEM image of 100-nm silver nanoparticles deposited on the gas diffusion layer.

ESI Method: Calculation of theoretical rate of CO₂ conversion to carbonates.

Only CO₂ dissolved in an aqueous environment would undergo the reaction with hydroxides, so the concentration of CO₂ dissolved in water at the electrode surface was calculated based on Henry's Law, as shown in the following equation:

$$[CO_2]_{aq} = H_{CO_2} P_{CO_2}$$

Since the concentration of CO₂ will continue to decrease as the gas travels along the serpentine channel, the log mean average CO₂ concentration was assumed for calculation as an approximate amount of how much CO₂ will be available for carbonate formation during the simultaneous electroreduction reaction, setting the initial pressure of CO₂ as 1 atm and the final partial pressure of CO₂ to reflect the lowest possible concentration of CO₂ in the outlet exiting the outlet. Although ideally we would want to have no CO₂ leftover in the effluent, we used a CO₂ partial pressure of 0.005 atm as the amount leftover after the entire reaction.

A modified Nernst-Planck equation relating ion flux to the current was used:

$$J_i = \frac{z_i C_i D_i}{n \sum_i z_i C_i D_i} \left(-\frac{I}{F} \right)$$

Where J_i represents the flux of species i across the membrane, D_i represents the diffusion coefficient of species i in an aqueous medium, F represents Faraday's constant, R represents the gas constant, T represents temperature, and z_i represents the valence of the ion.

At steady state, the reaction rate of carbonate formation is set equal to the total carbonate flux, represented by the Nernst-Planck equation. To determine the actual concentration of hydroxide at the electrode surface formed during the reaction, equilibrium constants, K1 and K2, and the water dissociation constant, kw, as shown below, were used to convert the concentration of bicarbonate and carbonate as expressions relating with the concentration of hydroxide.

$$K1 = \frac{[H^+][HCO_3^-]}{[CO_2]_{aq}} = \frac{kw[HCO_3^-]}{[OH^-][CO_2]_{aq}}$$

$$K2 = \frac{[H^+][CO_3^{2-}]}{[HCO_3^-]} = \frac{kw[CO_3^{2-}]}{[OH^-][HCO_3^-]}$$

In addition, we assumed charge conservation by setting the total anion concentration equal to that of the membrane, which represents the cation concentration. The cation concentration, C⁺, is given by taking the product of the specified ion exchange capacity of the membrane and the density of the membrane (ρ_{mem}). This charge conservation equation was also used to rearrange the bicarbonate concentration as an expression related to hydroxide.

$$C^+ = IEC \cdot \rho_{mem} = 2[CO_3^{2-}] + [HCO_3^-] + [OH^-]$$

With all these assumptions and substitutions of equations, we can calculate the steady state concentration of hydroxide, and as a result, we can calculate the concentrations of bicarbonate and carbonate. This will give us the total flux of carbonates and bicarbonates, which would give us the total amount of CO₂ that will react with hydroxides at the given current, using the constants listed in ESI Table 2.

References

1. Verma, S., Lu, X., Ma, S., Masel, R. I. & Kenis, P. J. A. The effect of electrolyte composition on the electroreduction of CO₂ to CO on Ag based gas diffusion electrodes. *Phys. Chem. Chem. Phys.* **18**, 7075–7084 (2016).
2. Dufek, E. J., Lister, T. E., Stone, S. G. & McIlwain, M. E. Operation of a Pressurized System for Continuous Reduction of CO₂. *J. Electrochem. Soc.* **159**, F514–F517 (2012).
3. Ma, S. *et al.* Carbon nanotube containing Ag catalyst layers for efficient and selective reduction of carbon dioxide. *J. Mater. Chem. A* **4**, 8573–8578 (2016).
4. Verma, S. Hamasaki, Y., Kim, C., Huang, W., Lu, S., Jhong, H. R. M., Gewirth, A. A., Fujigaya, T., Nakashima, N., Kenis, P. J. A. Insights into the Low Overpotential Electroreduction of CO₂ to CO on a Supported Gold Catalyst in an Alkaline Flow Electrolyzer. *ACS Energy Lett.* **3**, 193–198 (2018).
5. Ma, S., Lan, Y., Perez, G. M. J., Moniri, S. & Kenis, P. J. A. Silver supported on titania as an active catalyst for electrochemical carbon dioxide reduction. *ChemSusChem* **7**, 866–874 (2014).
6. Möller, T., Ju, W., Bagger, A., Wang, X., Luo, F., Ngo Thanh, T., Varela, A. S., Rossmeisl, J., Strasser, P. Efficient CO₂ to CO electrolysis on solid Ni-N-C catalysts at industrial current densities. *Energy Environ. Sci.* **12**, 640–647 (2019).
7. Salvatore, D. A., Weekes, D. M., He, J., Dettelbach, K. E., Li, Y. C., Mallouk, T. E., Berlinguette, C. P. Electrolysis of Gaseous CO₂ to CO in a Flow Cell with a Bipolar Membrane. *ACS Energy Lett.* **3**, 149–154 (2018).
8. Li, T., Lees, E. W., Goldman, M., Salvatore, D. A., Weekes, D. M., Berlinguette, C. P. Electrolytic Conversion of Bicarbonate into CO in a Flow Cell. *Joule* **3**, 1487–1497 (2019).
9. Gabardo, C. M., Seifitokaldani, A., Edwards, J. P., Dinh, C. T., Burdyny, T., Kibria, M. G., O'Brien, C. P., Sargent, E. H., Sinton, D. Combined high alkalinity and pressurization enable efficient CO₂ electroreduction to CO. *Energy Environ. Sci.* **11**, 2531–2539 (2018).
10. Dinh, C. T., García De Arquer, F. P., Sinton, D. & Sargent, E. H. High rate, Selective, and Stable Electroreduction of CO₂ to CO in Basic and Neutral Media. *ACS Energy Lett.* **3**, 2835–2840 (2018).
11. Weng, L.-C., Bell, A. T. & Weber, A. Z. Towards membrane-electrode assembly systems for CO₂ reduction: a modeling study. *Energy Environ. Sci.* **12**, 1950–1968 (2019).
12. Millero, F. J., Graham, T. B., Huang, F., Bustos-Serrano, H. & Pierrot, D. Dissociation constants of carbonic acid in seawater as a function of salinity and temperature. *Mar.*

- Chem.* **100**, 80–94 (2006).
13. Myles, T. D., Grew, K. N., Peracchio, A. A. & Chiu, W. K. S. Transient ion exchange of anion exchange membranes exposed to carbon dioxide. *J. Power Sources* **296**, 225–236 (2015).
 14. Kaczur, J. J., Yang, H., Liu, Z., Sajjad, S. D. & Masel, R. I. Carbon Dioxide and Water Electrolysis Using New Alkaline Stable Anion Membranes. *Front. Chem.* **6**, 263 (2018).
 15. Dighe, A. S. Imidazole. *Pharmaceutical Organic Chemistry* (2020).